Manifestations of pear-shaped clusters in collinear cluster tri-partition (CCT)

Yu.V. Pyatkov[1,2], D.V. Kamanin[2], A.A. Alexandrov[2], I.A. Alexandrova[2], Z.I. Goryainova[2], V. Malaza[3], E.A. Kuznetsova[2], A.O. Strekalovsky[2], O.V. Strekalovsky[2] and V.E. Zhuchko[2]

National Nuclear Research University MEPhI (Moscow Engineering Physics Institute), Moscow, Russia
Joint Institute for Nuclear Research, Dubna, Russia
University of Stellenbosch, Faculty of Military Science, Military Academy, Saldanha 7395, South Africa

Experimental background

Collinear cluster tri-partition (CCT) – status quo

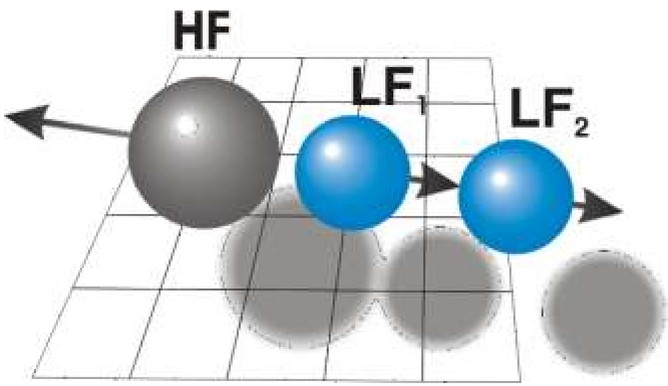

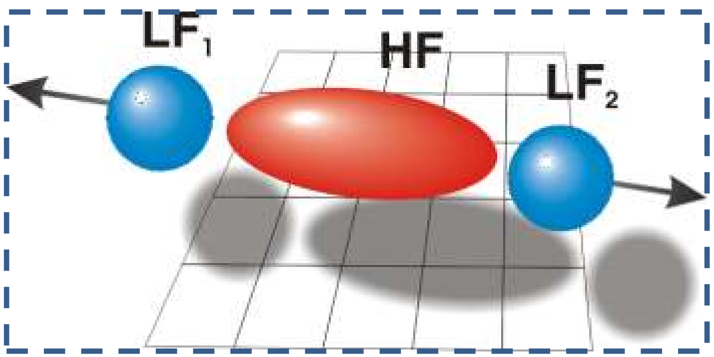

Prescission ternary configurations supposed to be in game

PHYSICAL REVIEW C 96, 064606 (2017)
Examination of evidence for collinear cluster tri-partition
Yu. V. Pyatkov,[1,2] D. V. Kamanin,[2] A. A. Alexandrov,[2] I. A. Alexandrova,[2] Z.
V. Malaza,[3] N. Mkaza,[3] E. A. Kuznetsova,[2] A. O. Strekalovsky,[2] O. V. Strekal
[1]National Nuclear Research University MEPhI (Moscow Engineering Physics Institu
[2]Joint Institute for Nuclear Research, Dubna, Russia
[3]University of Stellenbosch, Faculty of Military Science, Military Academy, Saldanha
(Received 10 August 2017; published 11 December 2017)
Background: In a series of experiments at different time-of-flight spectrometers of h
manifestations of a new at least ternary decay channel of low excited heavy nuclei. D

http://fobos.jinr.ru/

Our experimental background

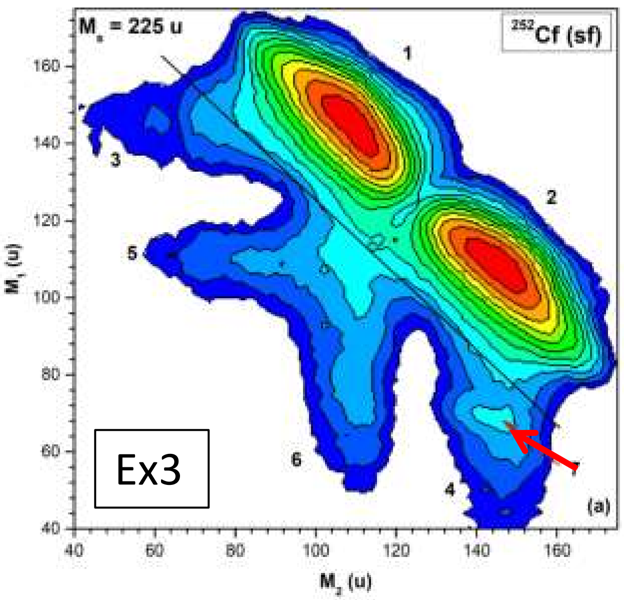

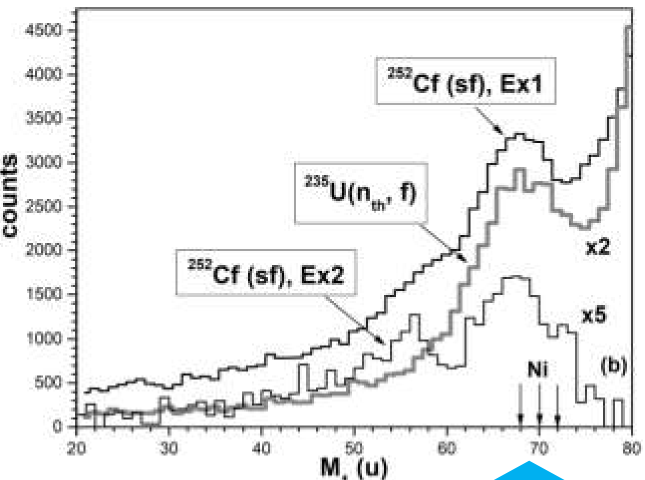

"Ni-bump"

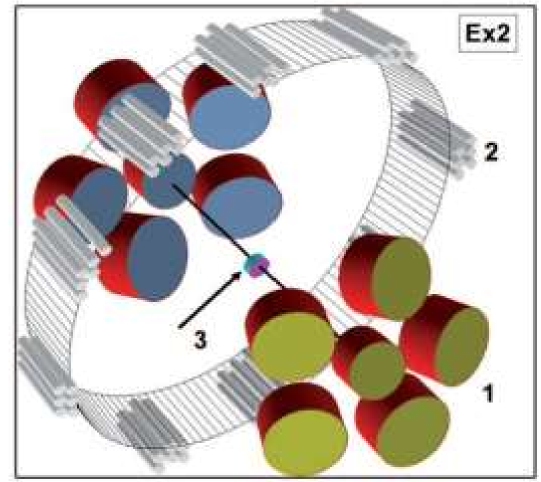

Mtt & Mte,
Neutrons &
Nuclear charge

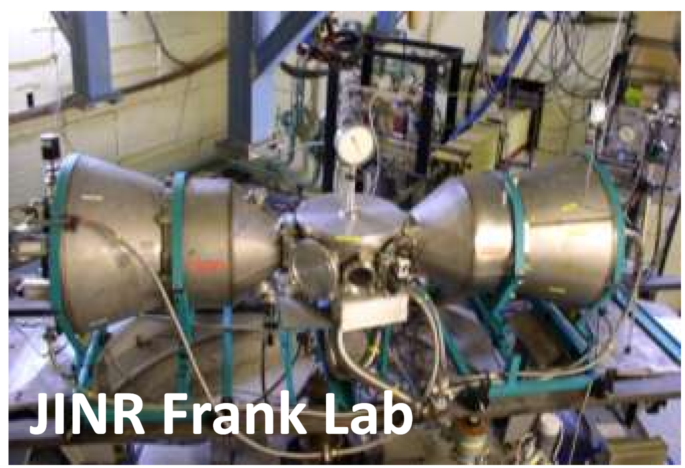

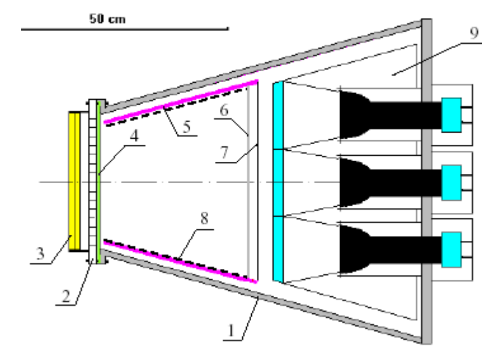

New modified experimental methodic

New experimental approach

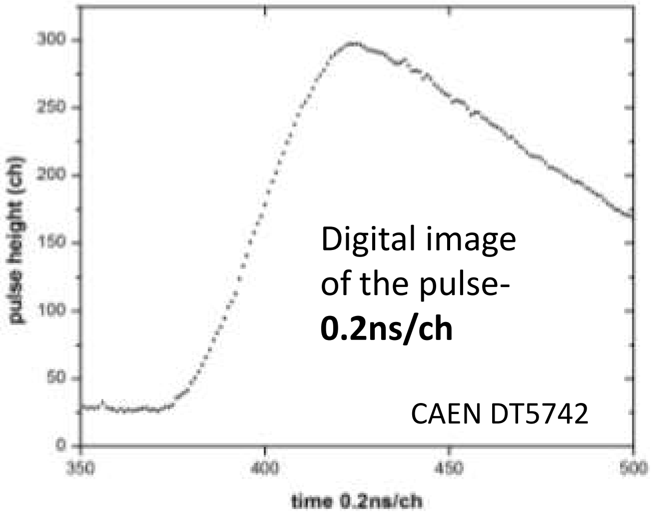

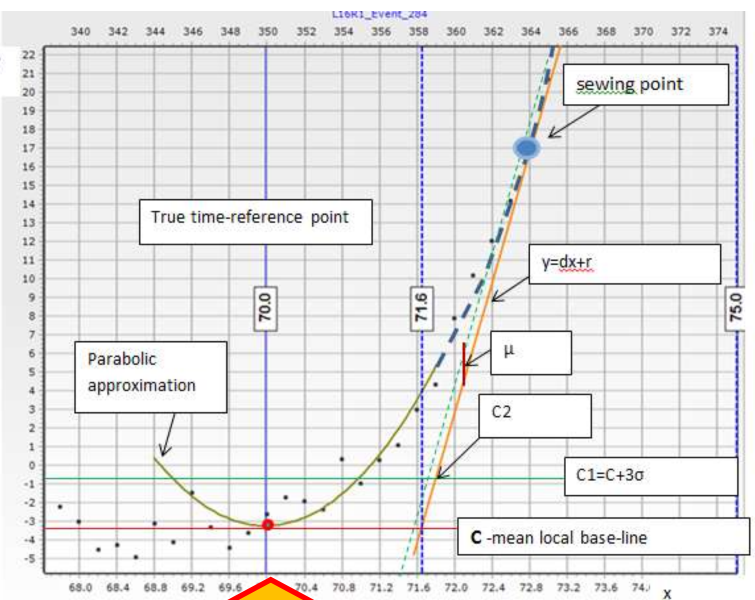

True time reference point

PHD:

$$E = E_{det} + R(M,E), \quad (1)$$

$$R(M,E) = \frac{\lambda \cdot E}{1 + \varphi \cdot \frac{E}{M^2}} + \alpha \cdot ME + \beta \cdot E, \quad (2)$$

$$E = \frac{M \cdot V^2}{1.9297} \quad (3)$$

$$\longrightarrow \quad G(\{\lambda, \varphi, \alpha, \beta\}, M, V) = 0$$

Combining equation (1), (2) and (3), we obtain:

$$G = \frac{MV^2}{k} - [E_{det} + \frac{\lambda \cdot \frac{MV^2}{k}}{1 + \varphi \cdot \frac{V^2}{Mk}} + \alpha \cdot \frac{M^2V^2}{k} + \beta \cdot \frac{MV^2}{k}] = 0,$$

where $k = 1.9297$.

$$\min \quad F = [(<ML_T> - <ML>)^2 + (<MH_T> - <MH>)^2] + \mu \sum_{M_{TE}} \frac{(Y(M_{TE}) - Y_T(M_{TE}))^2}{Y(M_{TE})}$$

PD:

$$\Delta t_p = \gamma \frac{M^{1/6} E^{1/2}}{\ }$$

A new off-line method of time-pickoff "sewing-parabola"

New results

Comparison of the results from Ex1 (new) and Ex2

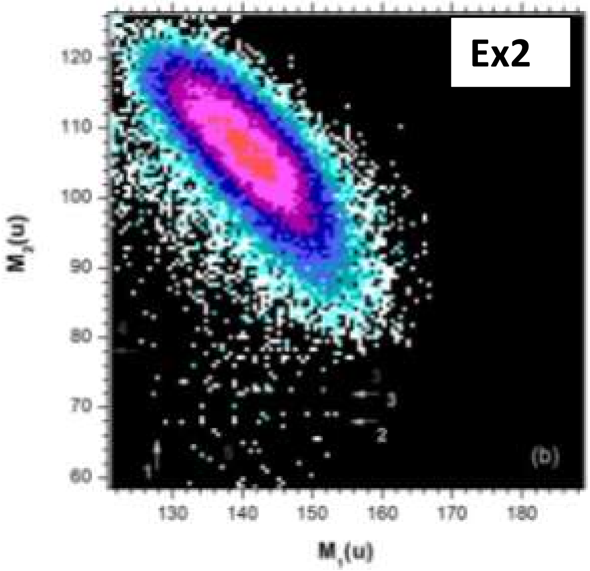

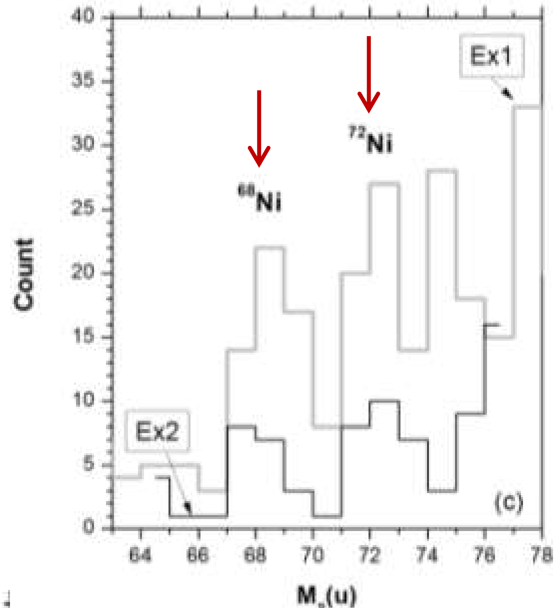

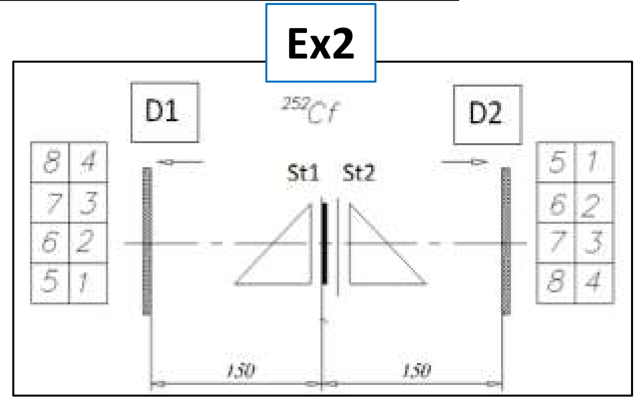

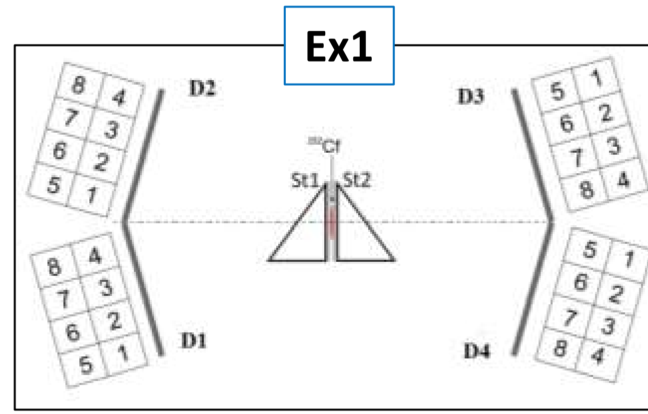

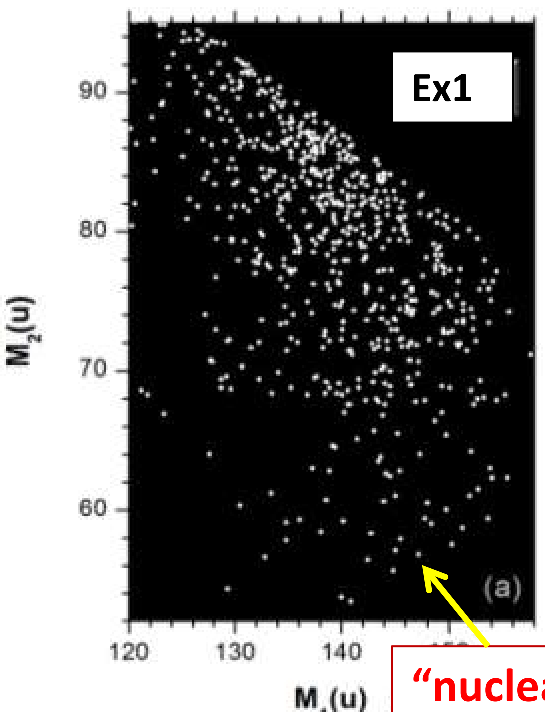

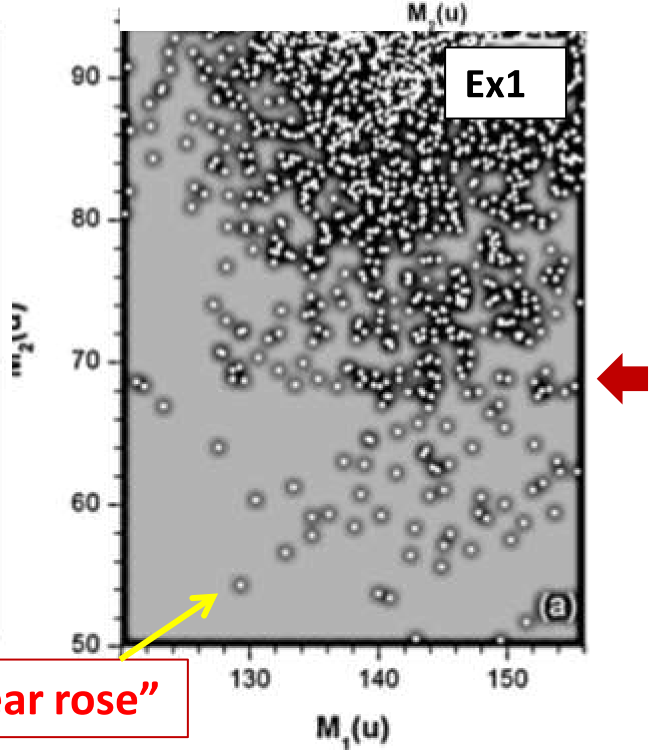

"nuclear rose"

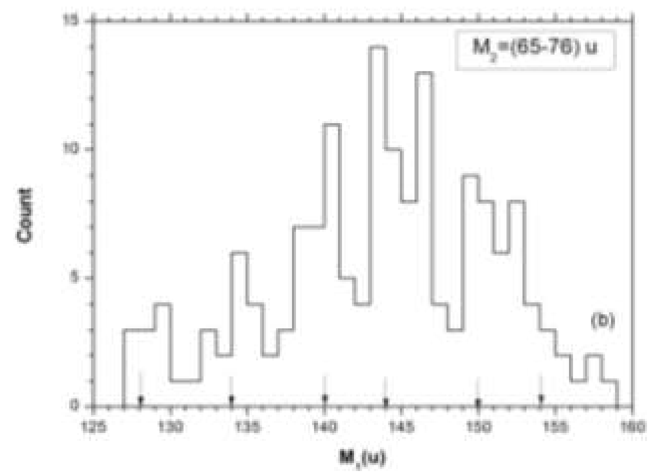

Structures under analysis: tilted lines M_1+M_2=const

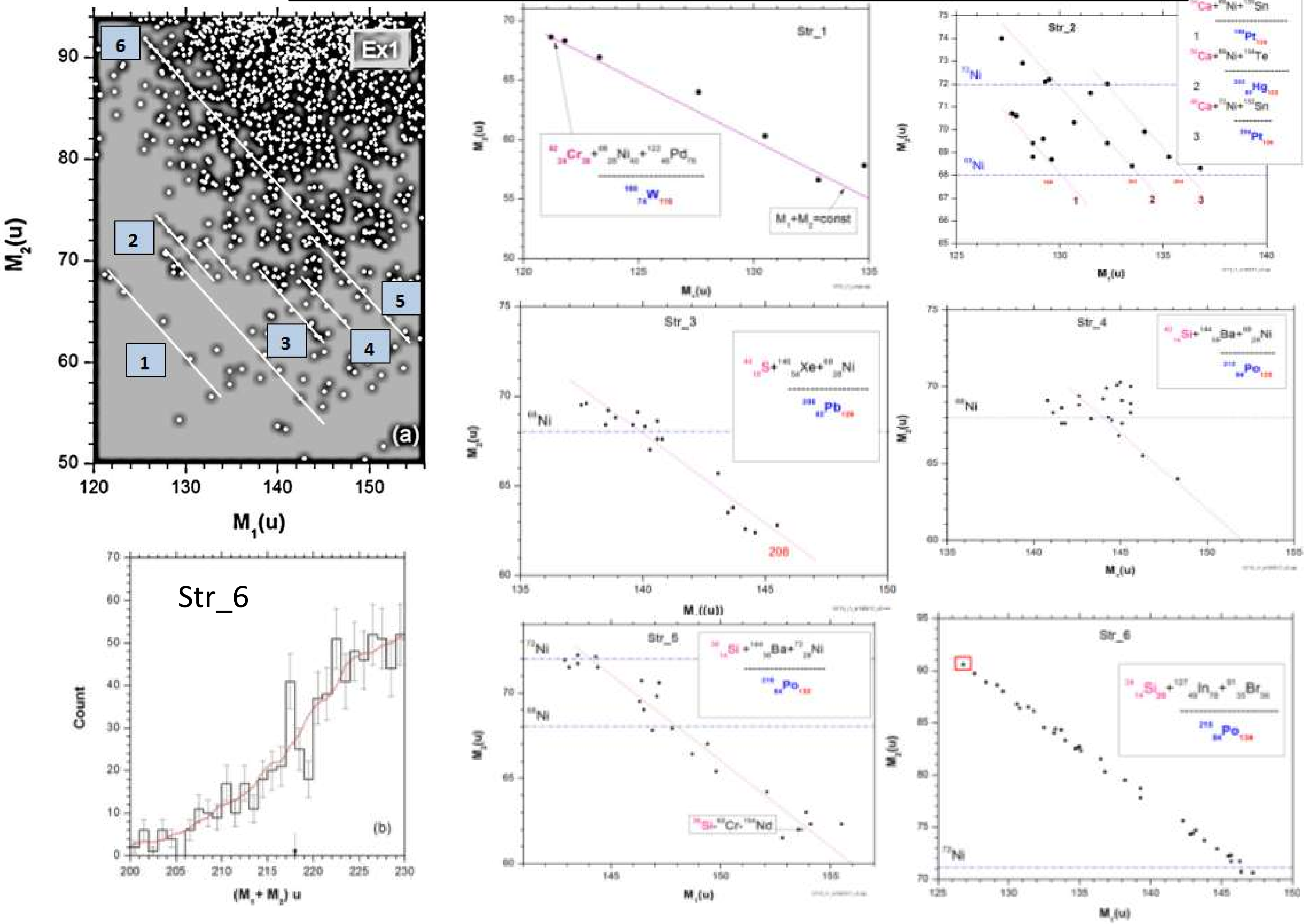

Three different experiments but similar structures

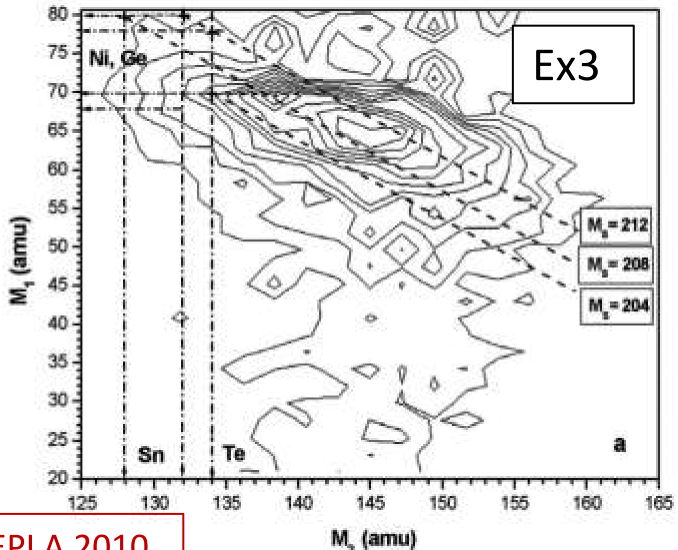

EPJ A 2010

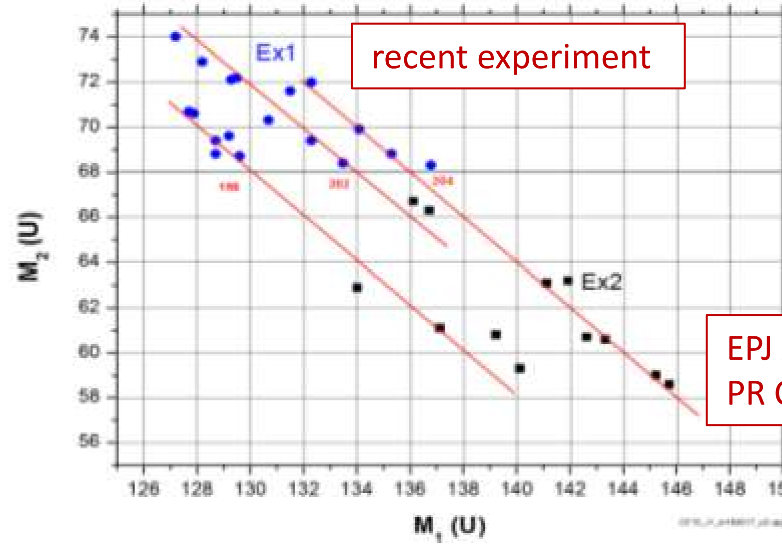

EPJ A 2012
PR C 2017

With the mosaics of PIN diodes

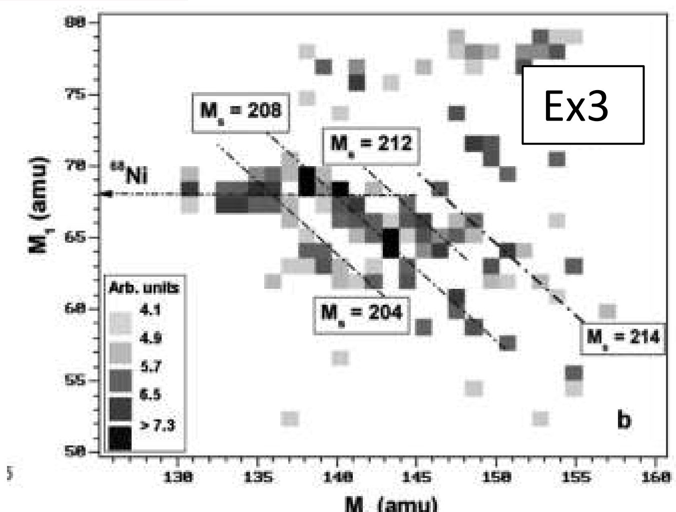

at FOBOS setup

Parameters of the structures observed

Str №	Missed fragment	Heavy magic core	Number of neutrons	Experiments
1	62Cr	190W	116	Ex1
2	48, 50, 54Ca	198Pt, 202Hg, 204Pt	120, 122, 124	Ex1 & Ex2
3	44S	208Pb	126	Ex1 & Ex3
4	40Si	212Po	128	
5	36S	216Po	132	
6	34Si (N=20)	218Po	134	Ex1

new

Discussion

Deformed magic core causes the effect

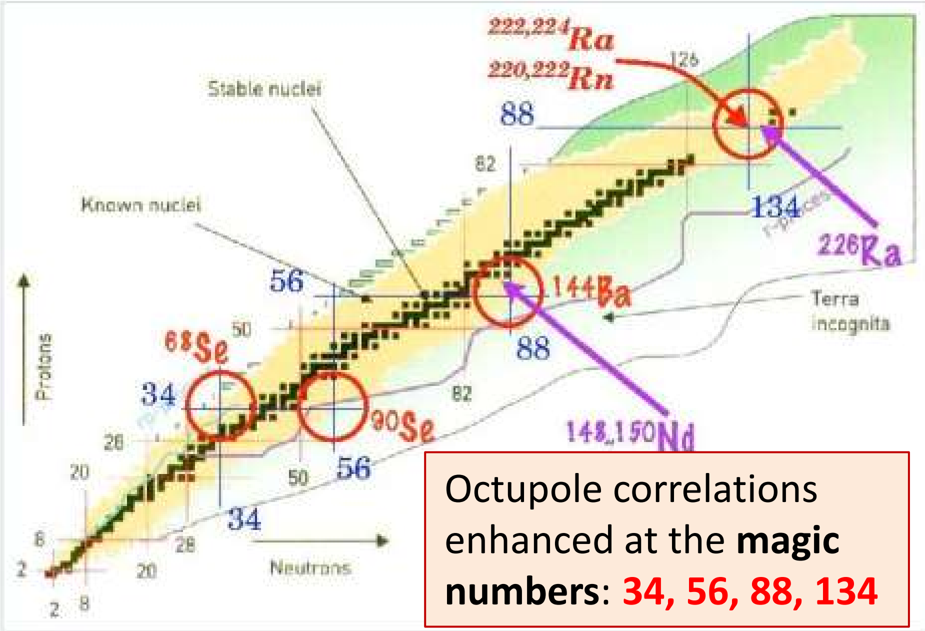

Octupole correlations enhanced at the **magic numbers**: **34, 56, 88, 134**

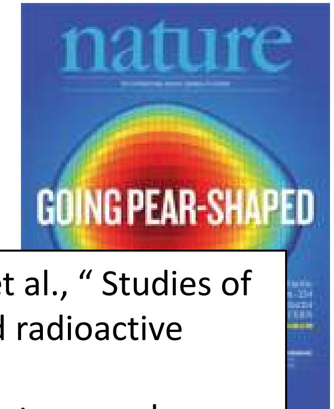

L. P. Gaffney, P. A. Butler, M. Scheck et al., " Studies of pear-shaped nuclei using accelerated radioactive beams", **Nature V497 (2013)**

"Strong octupole correlations leading to pear shapes can arise when nucleons near the Fermi surface occupy states of opposite parity with orbital and total angular momentum differing by 3h. This condition is met for proton number Z≈34, 56 and 88 and neutron number **N≈34, 56, 88 and 134.** The largest array of evidence for reflection asymmetry is seen at the values of Z≈88 and N≈134".

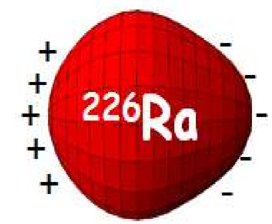

In an **octupole** deformed nucleus the center of mass and center of charge tend to separate, creating a non-zero **electric dipole moment**.

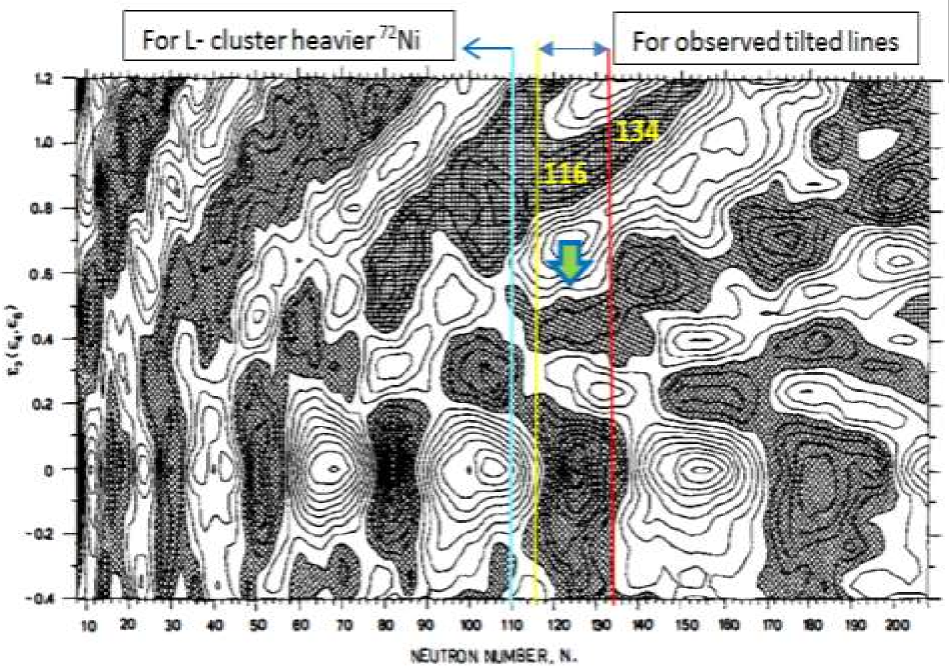

Heavy magic core	Number of neutrons
190W	116
198Pt, 202Hg, 204Pt	120, 122, 124
208Pb	126
212Po	128
216Po	132
218Po	134

S. Aberg, H. Flacard, W. Nazarewicz, Annu. Rev. Nucl. Part. Sci. 1990.40: 439-527

Presumable prescission shape of the nucleus in the mode under discussion

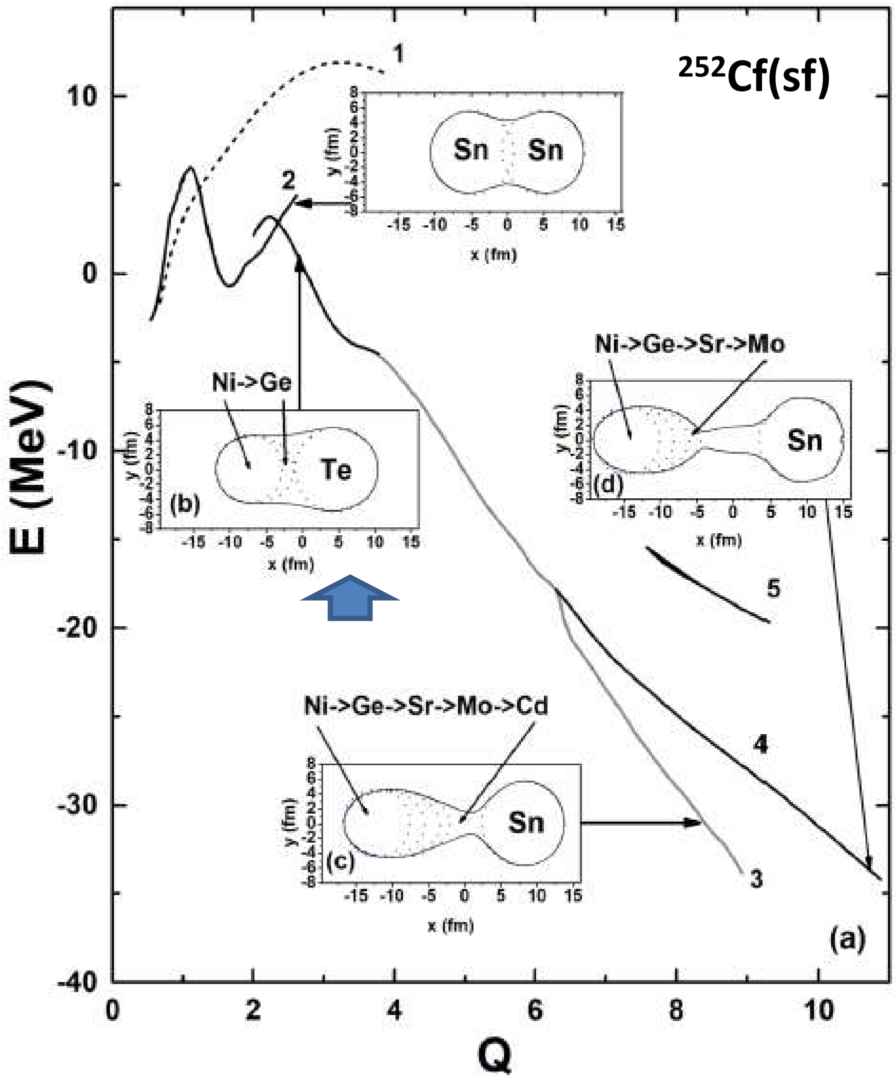

Yu. V. Pyatkov, V. V. Pashkevich, et al., Nucl. Phys. A 624, 140 (1997).

octupole deformed magic core

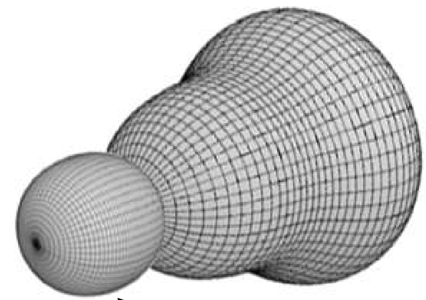

light cluster which manifests itself in experiment via missing mass

Energies of the detected fragments in Ex1 and Ex2

PHYSICAL REVIEW C 96, 064606 (2017)

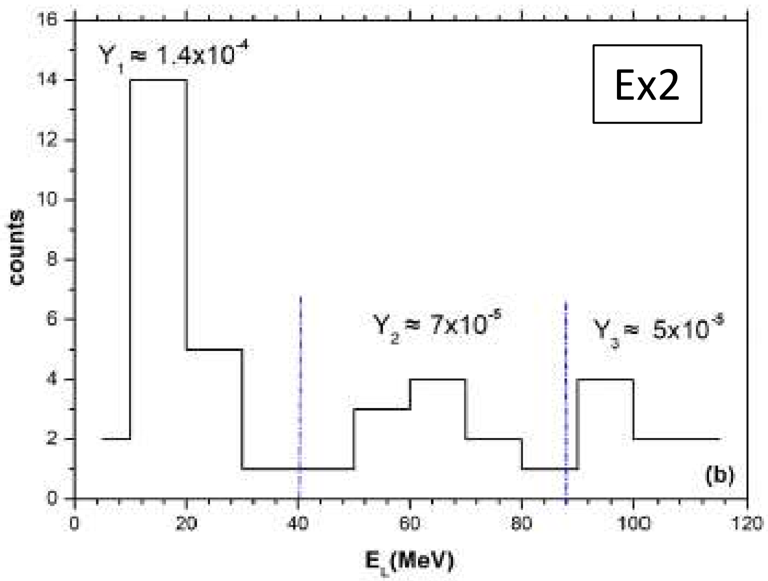

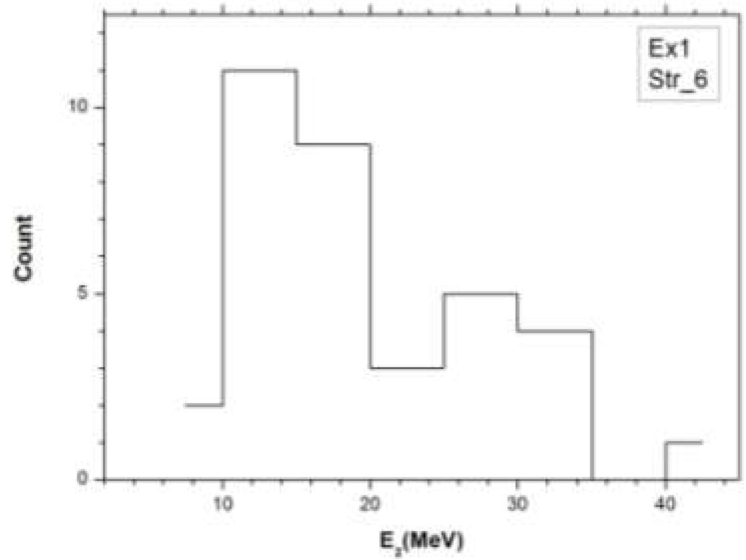

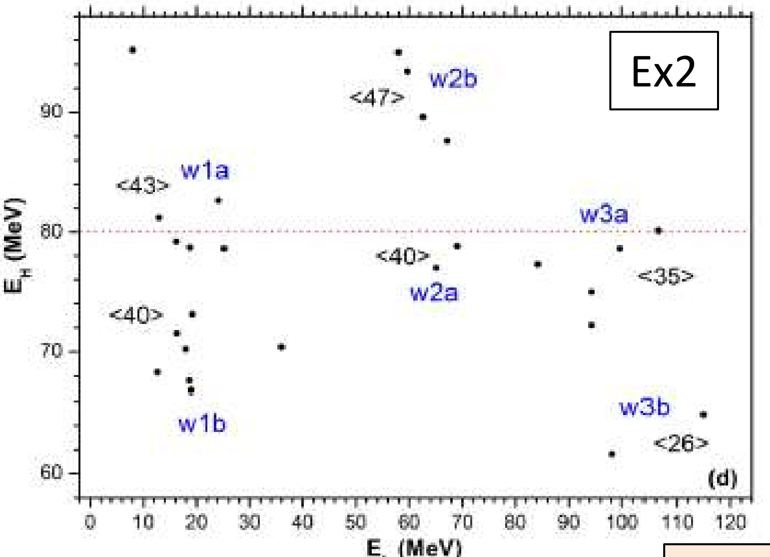

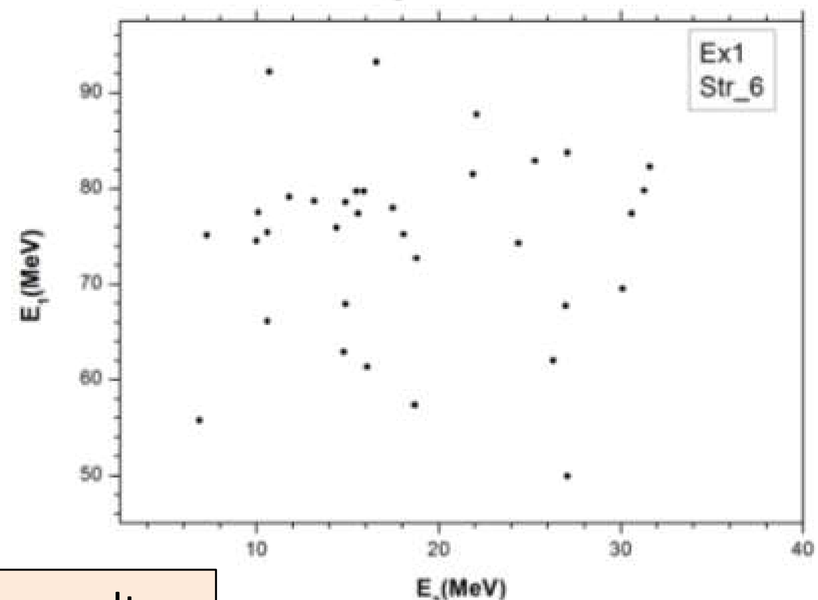

similar results

Scission scenario

Ex	Structure under analysis	System configuration at the exit point	System configuration after first rupture	System configuration at the moment of the second rupture
Ex1	Constant missing mass (M_3)	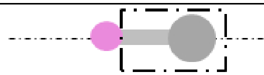 magic core	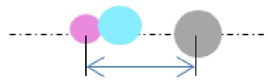	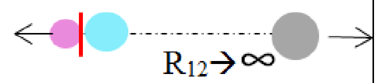
Ex2	“Ni-bump”	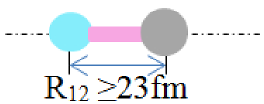 L&H magic clusters	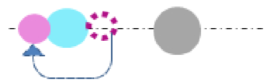	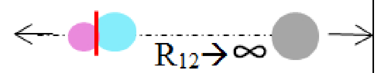

TABLE I. Results of the model calculations. Ternary partitions close to the experimental ones and based on magic constituents (marked in bold) are shown in square brackets. See the text for details.

No.	Locus	Nucl. configuration	R_{12}, fm	$E_{H\,\mathrm{sec}}$ MeV	E_H, MeV	V_L, cm/ns	$V_{L\,\mathrm{sec}}$, cm/ns	V_T, cm/ns
1	$w1b$	^{70}Ni–^{43}S–^{139}Xe [^{70}**Ni**–^{42}**S**–^{140}**Xe**]	⩽27	71	80.4 ± 1.8	0.71 ± 0.1		2.16 ± 0.06
2	$w1c$	^{70}Ni–^{39}Si–^{143}Ba [^{70}**Ni**–^{38}Si–^{144}**Ba**]	⩽30	58	69.5 ± 2.6	0.68 ± 0.06		2.19 ± 0.13
3	$w2b$	^{70}Ni–^{47}Ar–^{135}Te [^{72}**Ni**–^{46}**Ar**–^{134}**Te**]	⩽35		91.4 ± 3.1	1.30 ± 0.06	1.34	1.33 ± 0.22
4	$w2c$	^{70}Ni–^{40}S–^{142}Xe [^{70}**Ni**–^{42}**S**–^{140}**Xe**]	⩽35		77.9 ± 1.3	1.36 ± 0.03	1.34	1.31 ± 0.004
5	$w3b$	^{70}Ni–^{35}Al–^{147}La [^{70}**Ni**–^{34}Mg–^{148}**Ce**]	⩽32	60	76.6 ± 3.1	1.62 ± 0.04		0.78 ± 0.08
6	$w3c$	^{70}Ni–^{26}Ne–^{156}Nd [^{70}**Ni**–^{28}Ne–^{154}**Nd**]	⩽28	52	63.2 ± 2.3	1.68 ± 0.1		0.58 ± 0.05
7	bin. fiss.	^{70}Ni–^{50}Ca/^{132}Sn ^{182}Yb			TKE 141 MeV $E_{\mathrm{Ni}} = 102$ MeV			

Conclusion

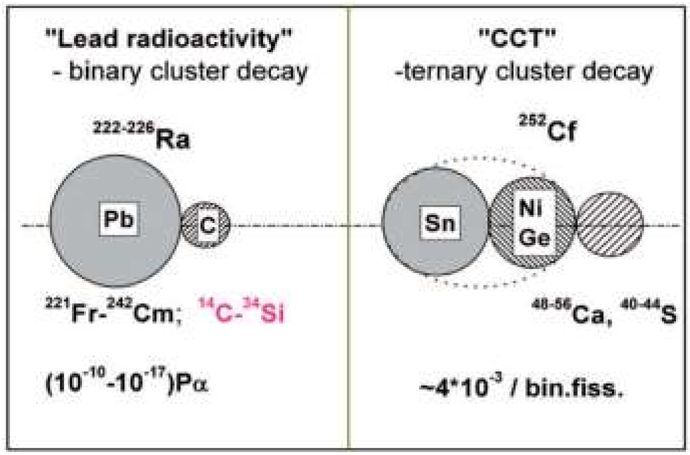

Fig. 10. Cluster scheme for the comparison of the lead radioactivity with collinear cluster tri-partition (Yu.V. Pyatkov et al., EPJ A 2010)

Basing on new data we clarify
a mechanism of the CCT mode
similar to heavy ion radioactivity,
namely,
octupole deformed magic core plays the same role as magic Pb in the "Lead radioactivity".